

# STUDY OF ENERGY JITTER AND ENERGY SPREAD COMPRESSION FOR THE CSNS-II LINAC\*

Y. Han<sup>†1,2</sup>, M. Huang<sup>1,2</sup>, A. Li<sup>1,2</sup>, Z. Li<sup>1,2</sup>, J. Peng<sup>1,2</sup>

<sup>1</sup>Institute of High Energy Physics, CAS, Beijing, China

<sup>2</sup>Spallation Neutron Source Science Center, Dongguan, China

## Abstract

The China Spallation Neutron Source (CSNS) is currently undergoing an upgrade to increase its beam power from 100 kW to 500 kW. As part of this enhancement, the linear accelerator's beam energy will be boosted from 80 MeV to 300 MeV, and the beam current will be raised from 10 mA to 40 mA. To achieve the higher beam energy, 52 superconducting cavities will be added following the drift tube linac. However, these new cavities are expected to increase both energy jitter and energy spread, potentially leading to significant beam loss during injection into the RCS ring. Therefore, it is crucial to carefully manage the energy jitter and energy spread. This paper first presents simulations of the beam energy jitter and energy spread at the end of the superconducting section with dynamic beam and cavities errors. Subsequently, it introduces a comparison of various compression schemes aimed at reducing energy jitter and energy spread.

## INTRODUCTION

The China Spallation Neutron Source (CSNS) is an accelerator-based neutron source located in Guangdong Province, China. Commissioning of CSNS began in 2017, and its design beam power of 100 kW was achieved in 2020. The accelerator complex consists of a linear accelerator providing a beam energy of 80 MeV and a Rapid Cycling Synchrotron (RCS) that accelerates the beam energy to 1.6 GeV [1, 2].

Since 2024, the CSNS-II upgrade project has been launched. The beam power will be increased to 500 kW, and two new application beamlines will be constructed. The main parameters of CSNS-II are listed in Table 1. To achieve a beam power of 500 kW, the beam current from the linac will be raised from 10 mA to 50 mA. Meanwhile, the beam energy at the linac exit will be increased to 300 MeV to mitigate the space-charge effect during injection into the RCS. The mitigation of instability has also been probably considered [3, 4].

Two types of superconducting cavities will be installed: spoke cavities and elliptical cavities, as illustrated in Fig. 1. The spoke cavities will accelerate the beam from 80 MeV to 165 MeV, with a total of 20 cavities arranged two per cryomodule. The elliptical cavities will boost the beam energy from 165 MeV to 300 MeV, with 24 cavities grouped three per cryomodule. Each cavity will be powered by an

independent RF source, resulting in a total of 44 power sources for the superconducting cavities. Significant jitter in beam energy and energy spread can be anticipated in such a linac system, which must be suitably compressed.

Table 1: The Main Parameters Of The CSNS-II

Project Phase	CSNS	CSNS-II
Beam Power [kW]	100	500
Energy [GeV]	1.6	1.6
Avg. Current [ $\mu$ A]	62.5	312.5
Peak Current at Linac [mA]	10	50
Pulse length [ $\mu$ s]	500	500
Duty Factor at Linac	1.25%	1.25%
RF Cavities at Linac	DTL	+Spoke+Ellip.
Number of Target	1	1
No. of Spectrometers	3	20

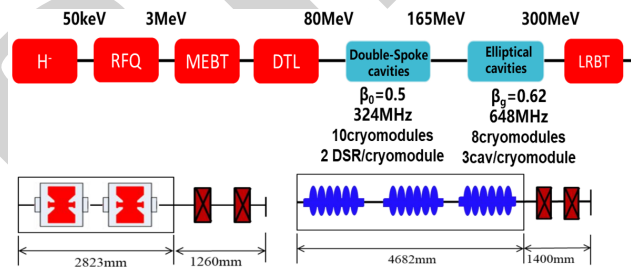


Figure 1: The layout of linac for the CSNS-II.

## THE REQUIREMENT FROM THE RCS

The long bunch pulse from the linac will be injected and accumulated into two bunches in the RCS, where constraints on beam energy and energy spread are imposed to improve injection efficiency. Simulations indicate that the momentum jitter  $\Delta p/p_0$  should be less than 0.2‰, and the energy spread jitter should be smaller than 1.0‰. For the 300 MeV beam delivered by the linac, this implies that the energy jitter must be controlled within 105 keV, and the energy spread must be limited to 527 keV.

## THE ERROR ANALYSIS FOR THE LINAC

The 44 accelerating cavities in the superconducting linac, together with the DTL, will inevitably introduce amplitude and phase errors and jitters, leading to fluctuations in both beam energy and energy spread at the exit of the superconducting section.

\* Work supported by the Open Fund of the China Spallation Neutron Source Songshan Lake Science City (Grant No. KFKT2023A01)T & IHEP talent foundation E15156U110.

<sup>†</sup> ylhan@ihep.ac.cn

An error analysis is first conducted to assess the energy jitter level at the exit of the superconducting cavities. Dynamical Gaussian distributed amplitude and phase errors are applied to all RF cavities, including the DTLs. The error levels are summarized in Table 2. Based on these error settings, 1000 random cases are simulated using the TRACEWIN code [5], with results presented in Fig. 2. It is found that the energy jitter can reach approximately 400 keV, far exceeding the RCS requirement of 105 keV. An energy jitter compression scheme must therefore be implemented in the downstream beamline. For the energy spread, simulations show that nearly all random cases remain below 400 keV, which is acceptable. Simulations also reveal that RF cavity errors can induce phase jitter on the order of  $\pm 2^\circ$  for the 324 MHz cavities, which may degrade the performance of energy jitter correction.

Table 2: RMS Amplitude And Phase Errors For RF Cavities

	DTL	Spoke	Elliptical
Amplitude [%]	0.17	0.1	0.1
Phase [deg]	0.1	0.1	0.1

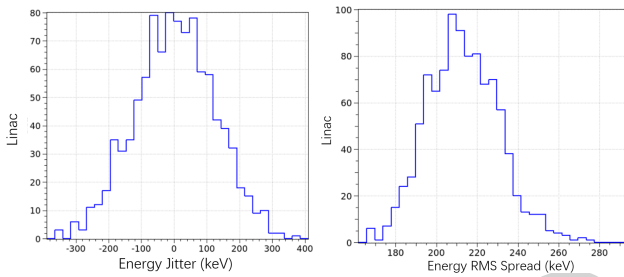


Figure 2: The error analysis considering all rf cavities errors for 1000 random machines. The left hand side plot shows the distribution of  $\Delta E$  and the right hand side plot shows the information about the energy spread.

## THE ENERGY JITTER CORRECTION SCHEME

The J-PARC linac faces a similar energy jitter issue, and a two-bunch correction system has been adopted to suppress it [6]. Simulations indicate that this system can reduce the energy jitter from a range of  $\pm 400$  keV to within  $\pm 200$  keV.

For CSNS-II, we have also investigated this correction scheme, whose layout is illustrated in Fig. 3. The available space downstream of the superconducting cavities in the linac tunnel is approximately 60 m. Under this constraint, the first debuncher is placed 16.8 m downstream of the superconducting cavity exit, i.e.,  $L1=16.8$  m. The second debuncher is positioned approximately 40 m upstream of the dipole bending magnet at the end of the linac.

We have also evaluated the single-debuncher scheme currently employed in our existing facility. In this configuration, the debuncher is located approximately 45 m downstream of the superconducting cavity exit.

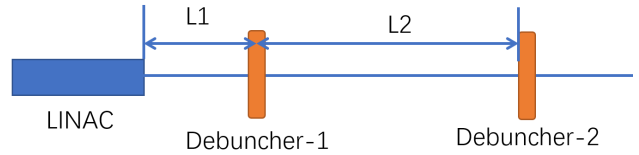


Figure 3: The schematic layout of the energy jitter correction for the CSNS-II.

## THE EFFECT OF THE TWO DEBUNCHERS

At the exit of the superconducting linac, there is no correlation between bunch energy and phase. In the two debuncher scheme, the first debuncher applies over-correction, allowing the second debuncher to control the energy spread independently.

In our design, the voltage is set to 3.3 MV for the first debuncher and 0.6 MV for the second. Under the error conditions listed in Tab. 2, the energy jitter can be corrected to approximately  $\pm 100$  keV as shown in Fig. 4. It should be noted that one case still exhibits an energy offset larger than 110 keV. The maximum energy spread is around 160 keV, which satisfies the requirements of the RCS.

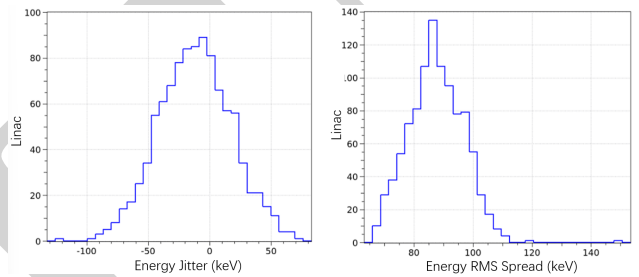


Figure 4: The energy jitter and energy spread after the 2 debuncher correction

It should be noted that the two-debuncher system assumes identical phases for different bunches at the exit of the RF cavities. In practice, however, erroneous bunches exhibit a phase difference of approximately  $\pm 2^\circ$ , which may degrade the correction performance. Figure. 5 shows the phase space  $\Delta E$  v.s.  $\phi$  at the end second debuncher, where the central phases are spread to  $\pm 4^\circ$ . In our facility, this effect is not problematic, as the resulting energy spread remains well below the required limit.

## THE EFFECT OF THE SINGLE DEBUNCHER

The single debuncher scheme is analogous to an energy compressor. The drift section establishes a correlation between beam phase and energy, while the debuncher acts to fully eliminate this correlation.

The final energy  $\delta_{E_f}$  after the debuncher can be expressed as:  $\delta_{E_f} = \frac{R_{65} \delta_{\phi_0} \beta \lambda}{2\pi} + (1 + R_{56} R_{65}) \delta_{E_0}$  [7]. Here,  $R_{56} = -\frac{L}{\gamma^2 \beta^2}$ ,  $R_{65} = -\frac{V \omega}{E \beta c}$ ,  $\beta$  and  $\gamma$  are the relativity velocity

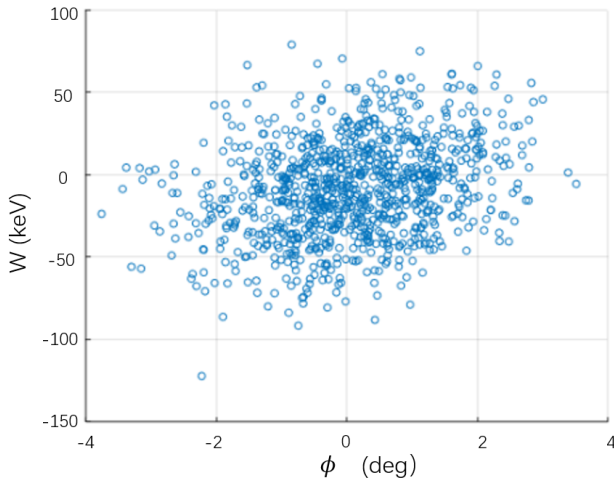


Figure 5: The  $\Delta E$  v.s.  $\phi$  after the correction with 2 debuncher scheme.

and Lorentz factor,  $V$  and  $\omega$  are the voltage and frequency of the debuncher, and the  $E$  is the reference beam energy.

Full compression implies that  $(1 + R_{56}R_{65}) = 0$ , such that the final energy jitter can be determined by the initial phase spread and the debuncher. At the end of the superconducting linac, there is no correlation between the beam center energy and the beam phase; as mentioned earlier, the beam phase jitters only within a narrow range of  $2^\circ$ . Therefore, the final energy jitter can be compressed to a very low level with a relatively small debuncher voltage. The debuncher voltage  $V$  is constrained by the full compression condition: a smaller voltage would require a larger  $R_{56}$ , which in turn necessitates a longer drift distance. However, the drift distance is limited by the accelerator layout, and we must avoid the heads and tails of adjacent bunches merging together after a long drift.

Following optimization, the drift length downstream of the superconducting cavities is set to 45 m, and the debuncher voltage is 0.85 MV. Figure 6 presents the energy jitter correction results using the single debuncher scheme for 1000 random machine cases. The energy jitter is constrained within a narrow range of  $\pm 30$  keV, and the energy spread is suppressed below 140 keV, which fully satisfies the requirements of the RCS ring.

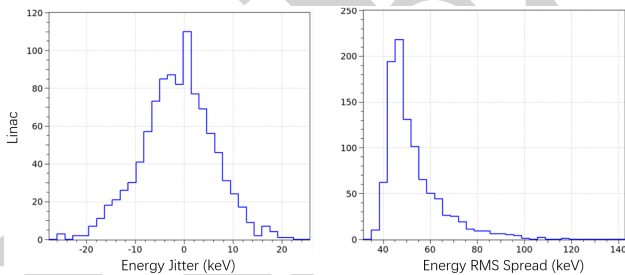


Figure 6: The energy jitter and energy spread after the single debuncher correction

Figure 7 shows the  $\delta E$  v.s. the phase for these 1000 random cases. The phases spans to a range about  $\pm 20$  degree, which is wider than the results using the two debuncher scheme. However, phase jitter is known to have negligible

impact on injection efficiency, so this degree of phase spread is acceptable.

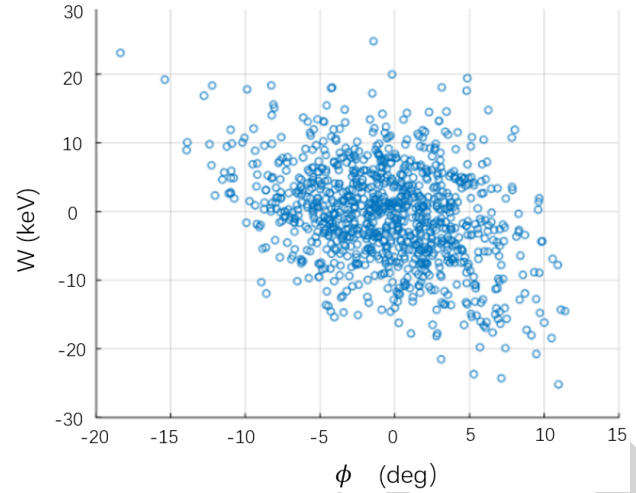


Figure 7: The  $\Delta E$  v.s.  $\phi$  after the single debuncher correction.

## ERRORS WITH OTHER DISTRIBUTION

We have also simulated other level of amplitude and phase jitter for the cavities in the linac as shown in Tab.3.

Table 3: Results For Different RF Jitter Levels

Type	Amp. [%]	Phase	E. Jitter and Spread
Gauss, 2 debnch	0.17	$0.1^\circ$	$\pm 100$ keV, 120 keV
Uni., 1 debnch	$\pm 0.5$	$\pm 0.3^\circ$	$\pm 50$ keV, 200 keV
Gauss, 2 debnch	0.34	$0.2^\circ$	$\pm 200$ keV, 130 keV
Gauss, 1 debnch	0.34	$0.2^\circ$	$\pm 60$ keV, 160 keV

These simulations indicate that the correction performance is sensitive to the random jitter levels. The error values presented in Table 2 are reasonable for our facility and will serve as the performance requirements for the RF system.

## SUMMARY

This paper investigates the energy jitter and energy spread jitter of the linac in the CSNS-II project. With more than 40 independent RF cavities, unavoidable energy and energy spread jitter will be introduced, which cannot be tolerated by the downstream RCS ring. Two correction schemes, employing two debunchers and a single debuncher, are simulated using 1000 random machine error cases. Simulation results demonstrate that both schemes can suppress the jitters to acceptable levels under the following conditions: DTL and superconducting cavities exhibit Gaussian-distributed amplitude jitter with RMS values of  $1.7\%$  and  $1.0\%$ , respectively, and phase jitter with an RMS of  $1.0\%$ . These levels represent realistic requirements for state-of-the-art low-level RF control systems.

## REFERENCES

- [1] S. Wang *et al.*, "An overview of design for CSNS/RCS and beam transport", *Sci. China Phys. Mech. Astron.*, vol. 54, suppl. 2, pp. s239–s244, 2011. doi:10.1007/s11433-011-4564-x
- [2] H. Chen *et al.*, "Design and construction of the China Spallation Neutron Source", *Nucl. Instrum. Methods Phys. Res. A*, vol. 1079, p. 170431, 2025. doi:10.1016/j.nima.2025.170431
- [3] L.-S. Huang *et al.*, "Pulsed octupole magnet for beam instability mitigation in rapid cycling synchrotron", *Nucl. Sci. Tech.*, vol. 37, p. 16, 2026. doi:10.1007/s41365-025-01853-7
- [4] L.-S. Huang *et al.*, "Impedance of RF shield on ceramic chamber in the rapid cycling synchrotron of China Spallation Neutron Source", *Nucl. Sci. Tech.*, vol. 37, p. 20, 2026. doi:10.1007/s41365-025-01856-4
- [5] D. Uriot and N. Pichoff, TraceWin. <http://irfu.cea.fr/Sacm/logiciels>
- [6] G. Wei and M. Ikegami, "Simulation study of debuncher system for J-PARC linac energy upgrade", in *Proc. LINAC'10*, Tsukuba, Japan, Sep. 2010, paper THP088. <https://jacow.org/LINAC2010/papers/THP088.pdf>, url = <https://jacow.org/LINAC2010/papers/THP088.pdf>
- [7] M. G. Minty and F. Zimmermann, *Measurement and control of charged particle beams*. Berlin, Germany: Springer, 2003. doi:10.1007/978-3-662-08581-3

PREPRINT